Received: 18 May 2024 | Revised: 8 July 2024 | Accepted: 29 July 2024

DOI: 10.1096/fj.202401119R

RESEARCH ARTICLE

The FASEB Journal

Hypoxia-inducible factor-1α can reverse the Adriamycin resistance of breast cancer adjuvant chemotherapy by upregulating transferrin receptor and activating ferroptosis

Xiaojie Yu[1] | **Qingqun Guo**[1] | **Haojie Zhang**[1] | **Xiaohong Wang**[2] | **Yong Han**[1] | **Zhenlin Yang**[1]

[1]Department of Thyroid Surgery, Binzhou Medical University Hospital, Binzhou, Shandong, P.R. China

[2]Department of Breast Surgery, Binzhou Medical University Hospital, Binzhou, Shandong, P.R. China

Correspondence
Yong Han and Zhenlin Yang, Department of Thyroid Surgery, Binzhou Medical University Hospital, Binzhou, Shandong 256603, P.R. China.
Email: hanyong2021@126.com and ikb0607@163.com

Funding information
National Natural Science Foundation of China, Grant/Award Number: 81902702; Natural Science Foundation of Shandong Province, Grant/Award Number: ZR2023MH115 and ZR2017LH072; National Key Research and Development Project, Grant/Award Number: 2018YFC0114705

Abstract

Breast cancer is a common malignant tumor in women. Ferroptosis, a programmed cell death pathway, is closely associated with breast cancer and its resistance. The transferrin receptor (TFRC) is a key factor in ferroptosis, playing a crucial role in intracellular iron accumulation and the occurrence of ferroptosis. This study investigates the influence and significance of TFRC and its upstream transcription factor hypoxia-inducible factor-1α (HIF1α) on the efficacy of neoadjuvant therapy in breast cancer. The differential gene obtained from clinical samples through genetic sequencing is TFRC. Bioinformatics analysis revealed that TFRC expression in breast cancer was significantly greater in breast cancer tissues than in normal tissues, but significantly downregulated in Adriamycin (ADR)-resistant tissues. Iron-responsive element-binding protein 2 (IREB2) interacts with TFRC and participates in ferroptosis. HIF1α, an upstream transcription factor, positively regulates TFRC. Experimental results indicated higher levels of ferroptosis markers in breast cancer tissue than in normal tissue. In the TAC neoadjuvant regimen-sensitive group, iron ion (Fe^{2+}) and malondialdehyde (MDA) levels were greater than those in the resistant group (all $p < .05$). Expression levels of TFRC, IREB2, FTH1, and HIF1α were higher in breast cancer tissue compared to normal tissue. Additionally, the expression of the TFRC protein in the TAC neoadjuvant regimen-sensitive group was significantly higher than that in the resistant group (all $p < .05$), while the difference in the level of expression of IREB2 and FTH1 between the sensitive and resistant groups was not

Abbreviations: ADR, adriamycin; BCA, bicinchoninic acid; CCK-8, cell counting kit-8; CR, complete response; DAB, diaminobenzidine; DEGs, differentially expressed genes; ECL, electrochemical luminescence; Fe^{2+}, iron ion; Fer-1, ferroptosis inhibitor; FTH1, ferritin heavy chain 1; GSH, glutathione; HIF1α, hypoxia-inducible factor-1α; IC50, cell viability and the half-maximal inhibitory concentration; IREB2, iron-responsive element-binding protein 2; IRES, iron-responsive element; KEGG, kyoto encyclopedia of genes and genomes; MDA, malondialdehyde; OD, optical density; OE-HIF1α, overexpressing HIF1α; PR, partial response; sh-HIF1α, downregulating the expression of HIF1α; sh-NC, nonsense sequence; TAC, docetaxel + adriamycin + cyclophosphamide; TFRC, transferrin receptor; WHO, World Health Organization.

Han Yong and Zhenlin Yang are co-corresponding authors.

significant ($p > .05$). The dual-luciferase assay revealed that HIF1α acts as an upstream transcription factor of TFRC ($p < .05$). Overexpression of HIF1α in ADR-resistant breast cancer cells increased TFRC, Fe^{2+}, and MDA content. After ADR treatment, the cell survival rate decreased significantly, and ferroptosis could be reversed by the combined application of Fer-1 (all $p < .05$). In conclusion, ferroptosis and chemotherapy resistance are correlated in breast cancer. TFRC is a key regulatory factor influenced by HIF1α and is associated with chemotherapy resistance. Upregulating HIF1α in resistant cells may reverse resistance by activating ferroptosis through TFRC overexpression.

KEYWORDS

Adriamycin resistance, breast cancer, ferroptosis, HIF1α, TFRC, transcription factor

1 | INTRODUCTION

Breast cancer is one of the most common malignancies among women. Adriamycin (ADR)-based chemotherapy regimens are commonly used as neoadjuvant treatments for HER2-negative breast cancer. However, ADR resistance and adverse drug reactions are major factors affecting the efficacy of breast cancer chemotherapy and can affect the clinical prognosis of patients.[1] Therefore, the mechanisms of drug resistance in breast cancer need to be elucidated to improve the prognosis of resistant patients. Iron ions help maintain the growth and metabolism of cells. Iron-mediated death, high iron metabolism, and ferroptosis in tumor cells not only influence the occurrence and development of tumors but are also closely associated with tumor resistance.[2] Ferroptosis is a form of cell death caused by high levels of iron-dependent intracellular lipid peroxidation,[3] with iron overload being the initiating factor for ferroptosis. Several factors influence iron ion metabolism, including the transferrin receptor (TFRC), which plays a crucial role in cellular iron transport. The expression of TFRC directly affects iron ion metabolism, making it an important regulator of ferroptosis.[4] Iron-responsive element-binding protein 2 (IREB2) is an important iron-responsive protein that affects iron levels by influencing the expression of the TFRC mRNA. Hypoxia-inducible factor-1α (HIF1α) is a nuclear protein that acts as a transcription factor and has many target genes. However, studies on its role in iron metabolism and its relationship with drug resistance in breast cancer are lacking.

In this study, we performed transcriptome sequencing, bioinformatics analysis, clinical validation, and cellular experiments to determine the changes in the expression of key factors involved in iron metabolism, including HIF1α, IREB2, TFRC, and ferritin heavy chain 1 (FTH1), as well as the iron death markers iron ion (Fe^{2+}), malondialdehyde (MDA), and glutathione (GSH). We analyzed their correlations, investigated the molecular mechanisms regulated by them, and assessed their effects on drug resistance. The findings of this study might provide new information that can be used to enhance the efficacy of neoadjuvant therapy for breast cancer.

2 | MATERIALS AND METHODS

2.1 | Materials

2.1.1 | Clinical samples

Tumor samples ($n = 150$) were collected from patients with invasive ductal carcinoma of the breast who were administered neoadjuvant TAC (docetaxel + ADR + cyclophosphamide) therapy at the Affiliated Hospital of Binzhou Medical University from 2018 to 2023. Complete clinical and pathological data were collected from the samples. Additionally, adjacent normal breast tissue samples were collected from the same patients. One part of each sample was fixed in a 4% formaldehyde solution and embedded in paraffin for histological analysis, while the other part was immediately snap-frozen in liquid nitrogen for further molecular studies. The inclusion criteria were as follows: (1) had invasive ductal carcinoma of the breast, diagnosed with breast cancer by two senior pathologists through a blind review, according to the 2019 World Health Organization (WHO) classification criteria for breast cancer; (2) had a negative HER2 status; (3) met the indications for neoadjuvant therapy; (4) were female primary patients who were ≥31 and ≤70 years old; (5) had not received prior treatment for breast cancer before neoadjuvant chemotherapy; (6) had undergone modified radical surgery after neoadjuvant chemotherapy; (7) had received six cycles of neoadjuvant chemotherapy before surgical treatment; (8)

had complete clinical and pathological data available. The exclusion criteria were as follows: (1) patients with distant metastases; (2) patients with other malignant tumors; (3) patients with severe concomitant diseases or other conditions that may interfere with planned treatment or comorbidities. According to the Response Evaluation Criteria in Solid Tumors (RECIST1.1),[5] among the 150 cases of invasive ductal carcinoma, 97 were TAC neoadjuvant-sensitive cases, and 53 were resistant cases. Among the 150 cases, 70 fresh samples were randomly selected (49 sensitive cases and 21 resistant cases). This study was approved by the Clinical Research Ethics Committee of Binzhou Medical University Affiliated Hospital, and all patients provided informed consent. In this study, 150 cases were included and the clinicopathological features are listed in Table S2. Among these 150 cases, 69 cases were younger than 50 years old. Fifty-one cases were presented with tumor of a diameter of over 5 cm. Based on clinical staging, 95 cases were classified as Stage I and II while 55 cases were classified as Stage III. According to histological grade, 108 cases were classified as Stage I and II while 42 cases were classified as Stage III. Lymph node metastasis was found in 98 cases. Eighty-five cases were found ER-positive whereas the number of PR-positive was 90. No case included in this study was found to be HER-2-positive.

2.1.2 | Reagents

The antibodies against β-actin (ab8226), TFRC (ab214039), IREB2 (ab232994), FTH1 (ab65080), and HIF1α (ab51608) were purchased from Abcam, United Kingdom. Immunohistochemistry kits, Western blot kits, and secondary antibodies (goat anti-rabbit/mouse IgG) were purchased from Shanghai Biyun Tian Biotechnology Co., Ltd. The qRT-PCR reagent kits were purchased from Beijing Takara Biotechnology Co., Ltd., and Takara synthesized specific primer sequences. Fe^{2+}, MDA (lipid peroxidation product), and GSH detection kits, FerroOrange fluorescence staining kits, cell proliferation and cell counting kit-8 (CCK-8) reagent kits, Fer-1 (ferroptosis inhibitor) reagent kits, and Erastin (ferroptosis activator) reagent kits were purchased from GlpBio, United States. Specific lentiviral sequences targeting the HIF1α gene and nonsense sequences were designed and provided by Shanghai Jikai Gene Medical Technology Co., Ltd.

2.1.3 | Cells

The human breast cancer cell lines, BT-549, BT-20, BT-474, HCC1954, MCF-7, and MDA-MB-435, were purchased from Wuhan Purnois Life Sciences Co., Ltd.

2.2 | Methods

2.2.1 | Tumor response grading criteria

Tumor response was assessed following the Response Evaluation Criteria in Solid Tumors (RECIST 1.1) after neoadjuvant chemotherapy and classified into sensitive and resistant groups. Among the 150 cases of invasive ductal carcinoma, 97 cases achieved complete response (CR) and partial response (PR); these cases were included in the TAC neoadjuvant-sensitive group. The remaining 53 cases were included in the TAC neoadjuvant-resistant group, which included cases with disease progression (CR) and stable disease (PR).

2.2.2 | Establishment of database and screening of differential genes

Three sensitive cases and three resistant cases were randomly selected for gene sequencing, which was performed by Guangzhou Ruibo Biotechnology Co., Ltd. RNA-Seq transcriptome data were obtained from one randomly selected group of sensitive and resistant cases. Differential target genes were screened, and the Kyoto Encyclopedia of Genes and Genomes (KEGG) pathway enrichment analysis was performed.

2.2.3 | Bioinformatics analysis

Based on the GEPIA database (http://gepia.cancer-pku.cn/), the expression of target genes in different tumors was analyzed. Additionally, using the TCGA data set in the UALCAN database (http://ualcan.path.uab.edu/index.html), the differences in the expression of target genes between breast cancer tissues and normal tissues were analyzed. Transcriptome data from the GSE50948 data set in the GEO database were downloaded to analyze the differential expression of target genes in neoadjuvant chemotherapy regimens based on ADR. The STRING database (https://www.string-db.org/) was used to construct a protein–protein interaction network of target genes and predict proteins that interact with target proteins. Transcriptome data corresponding to the TCGA-BRCA cohort were downloaded from the TCGA database, and the Spearman correlation coefficient was used to evaluate human transcription factors related to the expression of target genes in the data set. The promo tool was used to predict transcription factors related to target genes, and the Cytoscape software was used for visualization. Transcriptome data from the GSE50948 data set in the GEO database were downloaded to analyze the

transcription factors related to the differential expression of target genes in neoadjuvant chemotherapy regimens based on ADR.

2.2.4 | Detection and interpretation of Fe^{2+}, MDA, and GSH levels

The Fe^{2+} levels were measured using an iron ion detection kit, and MDA levels were determined using an MDA detection kit from both types of breast tissues (cancerous and normal breast tissues) and both types of breast cancer cells (sensitive and drug-resistant experimental cells). GSH levels were quantified using a GSH assay kit, and the differences in Fe^{2+}, MDA, and GSH levels between different groups were compared after the average OD values were calculated. The FerroOrange fluorescent probe kit was used to detect intracellular Fe^{2+} levels; red fluorescence in the cytoplasm was considered to indicate Fe^{2+} positivity, and the average light density was calculated.

2.2.5 | Immunohistochemistry EnVision method and interpretation of the results

Paraffin-embedded samples were cut into thin sections and deparaffinized in water. Antigen retrieval was performed using ethylenediaminetetraacetic acid (EDTA), and endogenous peroxidase activity was blocked with 3% H_2O_2. Next, the sections were incubated with primary antibodies overnight at 4°C, followed by incubation with secondary antibodies for 30 min at 37°C. The sections were treated with diaminobenzidine (DAB) for color development, after which the sections were counterstained with hematoxylin. Then, they were dehydrated, cleared, and mounted with neutral resin. Positive controls included tissues known to be positive for TFRC (esophageal cancer), IREB2 (lung cancer), FTH1 (normal liver tissue), and HIF1α (colon cancer). PBS was used instead of primary antibodies as a negative control.

Among the studied proteins, TFRC is primarily expressed in the cell membrane and cytoplasm, while IREB2 and FTH1 are mainly expressed in the cytoplasm. HIFα is mainly expressed in the cytoplasm and nucleus. Positive staining was indicated by a brownish-yellow color. To avoid bias and inaccuracies associated with subjective interpretation, quantitative interpretation of the markers was performed using the Image Pro Plus software to detect their optical density (OD) and calculate the average OD value. Samples with OD values greater than the average were considered to be positive; otherwise, they were considered to be negative.

2.2.6 | Cell culture and selection

The human breast cancer cell lines, BT-549, BT-20, BT-474, HCC1954, MCF-7, and MDA-MB-435, were seeded in RPMI-1640 medium supplemented with 10% fetal bovine serum and 1% antibiotics and cultured in a CO_2 incubator at 37°C, with an atmosphere containing 5% CO_2. The cells were passaged or the medium was changed based on the growth status of the cells. Western blotting analysis was performed to determine the expression of HIF1α in each cell line. The cells with high and low expression of HIF1α were selected as experimental cell lines.

2.2.7 | Western blotting

Cells (or tissues) were collected and lysed in RIPA buffer at 4°C. The cells were centrifuged, and the supernatant was collected. Next, the protein concentration was determined using the bicinchoninic acid (BCA) method. The obtained proteins were analyzed via gel electrophoresis, transferred to a membrane, and blocked. Primary antibodies were added to the samples, which were then incubated overnight at 4°C. The following day, the samples were incubated with secondary antibodies (goat anti-rabbit IgG) at room temperature, and then, electrochemical luminescence (ECL) was used for visualization. The ImageJ software was used to analyze the absorbance values of the target protein and β-actin. The relative level of expression of the target protein was calculated as the grayscale value of the target protein divided by the grayscale value of β-actin.

2.2.8 | qRT-PCR

After extracting RNA from the target cells (or tissues) using an RNA extraction kit, the RNA concentration was determined. RNA was reverse-transcribed into cDNA by conducting the corresponding reaction at 37°C for 15 min and 85°C for 5 s. PCR was performed using the SYBR Green relative quantitative PCR method. A reaction system of 25 μL was prepared according to the instructions provided with the kit and amplified using a CFX96T RT-PCR Detection System C1000 (Table S1). The reaction conditions were as follows: 95°C, 30 s; GOTO 39 (40 cycles in total); 95°C, 5 s; 60°C, 30 s. The relative level of expression of the sample was determined using the $2^{-\Delta\Delta Ct}$ method, where $\Delta\Delta Ct = \Delta Ct$ of the experimental group $- \Delta Ct$ of the blank or control group and $\Delta Ct = Ct$ value of the target gene $- Ct$ value of β-actin. The results are expressed as the average of three independent experiments.

2.2.9 | CCK-8 experiment

Cell suspensions were prepared and seeded at a density of 1×10^3 cells per well in a 96-well plate. Then, culture media containing different concentrations of ADR were added. After 24 h of incubation, the culture medium was discarded, and 10 μL of the CCK-8 solution was added to each well. The plate was then incubated at 37°C, and the OD of each well was measured at 450 nm using a microplate reader. This process was repeated three times. Cell viability and the half-maximal inhibitory concentration (IC50) were calculated. The dose–response curve was plotted based on cell viability and drug concentration.

2.2.10 | Cell invasion assay (Transwell assay)

The Matrigel matrix gel was mixed with RPMI-1640 medium and added to the upper chamber of Transwell inserts, followed by incubation at 37°C for 3 h. In each well of a 24-well plate, 800 μL of serum-containing medium was added to prepare a cell suspension at a density of 2×10^5 cells/mL. Then, 200 μL of the cell suspension was added to the Transwell inserts and incubated for 48 h. Non-migrating cells were removed, and the remaining cells were fixed with methanol and stained with Giemsa stain. The number of cells that migrated through the membrane was counted under a microscope. Three random fields per insert were analyzed, and the average number of migrated cells per field was calculated. The experiment was performed in triplicate.

2.2.11 | Cell proliferation assay (Plate clone formation assay)

Cells in the logarithmic growth phase were seeded at a density of 500 cells/well in a six-well plate and cultured with a medium for 1 week. When cell colonies were visible, the culture was terminated. The cells were fixed with methanol, stained with Giemsa stain, and then, counted and photographed under a microscope (magnification: 100×). Three random areas per well were analyzed, and the experiment was repeated three times.

2.2.12 | Experiment to verify the relationship between sensitivity of breast cancer cells to ADR and ferroptosis

To verify the relationship between the sensitivity of breast cancer cells (including sensitive cells, drug-resistant cells, and transfected cells) to ADR and ferroptosis, we conducted ferroptosis validation experiments using the ferroptosis inhibitor Fer-1 and the ferroptosis activator Erastin. Rescue experiments were conducted with Fer-1 intervention in the drug-sensitive cell lines, while activation experiments were conducted with Erastin intervention in the drug-resistant cell lines. Several groups were established, including the saline group, ADR group, intervention agent group, and ADR + intervention agent group. The CCK-8 assay was performed to determine cell viability and IC50 values of each group to assess the effect of ferroptosis on the sensitivity of breast cancer cells to ADR.

2.2.13 | Dual-luciferase assay

The dual-luciferase assay was conducted with technical support from Genecreate (Wuhan, China). This assay was performed to validate the transcriptional regulatory relationship between HIF1α and TFRC.

2.2.14 | Lentiviral transfection experiment for HIF1α intervention in cell lines

Two specific sequences targeting the HIF1α gene were designed and synthesized: one for downregulating the expression of HIF1α (sh-HIF1α) and the other for overexpressing HIF1α (OE-HIF1α). Additionally, one nonsense sequence (sh-NC) was designed as a negative control. The selected cell lines with high expression of HIF1α were divided into three groups, including the control group (no intervention), the sh-NC group, and the sh-HIF1α group. The cell lines with low expression of HIF1α were divided into the control group, sh-NC group, and OE-HIF1α group. Lentiviral transfection was conducted, and successful transfection was confirmed by Western blotting and qRT-PCR experiments to ensure successful intervention for subsequent experiments.

2.2.15 | Experiment on the effect of HIF1α intervention on ferroptosis-related factors in cell lines and its combined effect with ADR on cell survival

The selected and successfully transfected cell lines were subjected to Western blotting and qRT-PCR experiments to assess the expression of TFRC. Additionally, the levels of ferroptosis-related factors were measured using assay kits to analyze the effect of HIF1α intervention on the regulation of ferroptosis by TFRC.

Transfected cells that successfully underwent transfection were divided into two groups: the physiological

saline group and the ADR treatment group. Each group was treated with culture medium containing the respective half-maximal inhibitory concentration of ADR. The control group received an equal amount of physiological saline. The cells were cultured for 24 h, and the cell viability and IC50 values of each group were determined using the CCK-8 assay.

2.3 | Statistical analysis

All data were analyzed using the SPSS 26.0 software. All experiments were performed in triplicate with at least three independent samples. GraphPad Prism 8.0 and ImageJ were used to process images and data. Continuous data were expressed as the mean ± standard deviation ($\bar{x} \pm s$), and the differences in parameters between groups were determined by independent samples *t*-tests. Categorical data were expressed as *n* (%) and analyzed using the chi-squared test. The correlations between variables were assessed by performing Spearman correlation analysis and linear regression analysis. Cox proportional-hazards regression models were used to perform multivariate survival analysis. All results were considered to be statistically significant at $p < .05$.

3 | RESULTS

3.1 | Gene sequencing of clinical samples and identification of differential genes

Clinical samples comprising 37 364 genes were sequenced to obtain RNA-Seq transcriptome data. Among them, 874 genes were significantly differentially expressed ($p < .05$). By conducting *q*-value correction, 27 differentially expressed genes (DEGs) were identified ($q < .05$). The results of the KEGG pathway functional enrichment analysis revealed enrichment of TFRC in the iron death pathway among the DEGs. Additionally, the level of expression of the TFRC mRNA was significantly lower in resistant cases than in sensitive cases ($p < .05$, Figure 1A).

3.2 | Bioinformatics analysis of the relationship between TFRC and breast cancer

Based on the analysis conducted in the GEPIA database, TFRC expression differed significantly across 33 types of cancers, including breast cancer (Figure 1B). Using the UALCAN database, we found that the expression of the TFRC gene was upregulated in breast cancer tissues compared to that in normal breast tissues (Figure 1C). Analysis of the data from the GEO database illustrated the distribution of DEGs in the whole transcriptome profile, demonstrating significant downregulation of the TFRC gene in cases resistant to ADR-based chemotherapy (Figure 1D). Using the STRING database, a protein–protein interaction network of TFRC was constructed, and the top 10 proteins interacting with TFRC were identified. Among these proteins, IREB2 and FTH1 are related to ferroptosis, and interactions among them have been reported (Figure 1E).

To identify the factors that may influence the expression of TFRC, we predicted potential regulatory factors affecting the transcription of the TFRC gene based on the TCGA database. By intersecting with transcription factors, we found that HIF1α is a positive regulator of TFRC (Figure 1F). Analysis of the data from the GEO database revealed significant downregulation of the transcription factor HIF1α in cases resistant to neoadjuvant chemotherapy based on ADR (Figure 1D). Based on these findings, we further investigated the relationship between breast cancer resistance and ferroptosis, focusing on the regulatory mechanisms involving HIF1α and TFRC.

3.3 | Clinical sample validation of the relationships between HIF1α, TFRC, and Their related factors and breast cancer resistance

3.3.1 | Expression of HIF1α, IREB2, TFRC, FTH1, and ferroptosis markers in normal breast tissue and breast cancer

The results of the immunohistochemical analysis revealed that in the collected breast cancer tissue samples, the

FIGURE 1 Bioinformatics analysis. (A) Differential gene expression obtained from RNA-Seq transcriptomic data. Twenty-seven differentially expressed genes (DEGs) were identified ($q < .05$). (B) Analysis based on the GEPIA database reveals differential expression of transferrin receptor (TFRC) across 33 types of cancer, including breast cancer. (C) The UALCAN database indicates significant upregulation of the TFRC gene in breast cancer tissues. (D) Using the GSE50948 data set from the GEO database, TFRC and hypoxia-inducible factor-1α (HIF1α) exhibit significant downregulation in chemotherapy-resistant cases based on Adriamycin (ADR)-based therapy. (E) Constructing the TFRC protein interaction network in the STRING database reveals iron-responsive element-binding protein 2 (IREB2) and ferritin heavy chain 1 (FTH1) as interacting proteins with TFRC. (F) Prediction from the TCGA database suggests HIF1α as a positive regulatory transcription factor for TFRC.

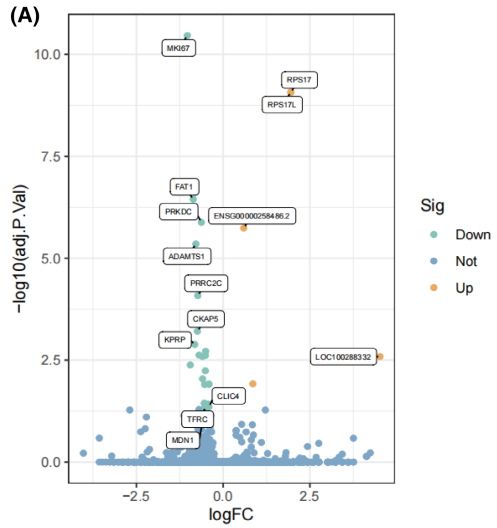

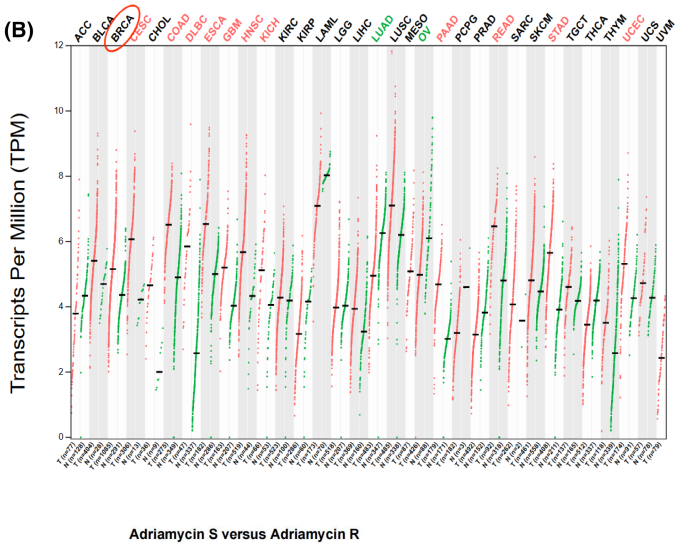

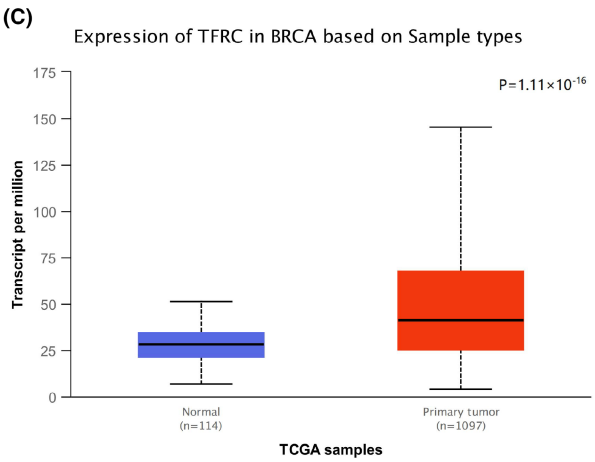

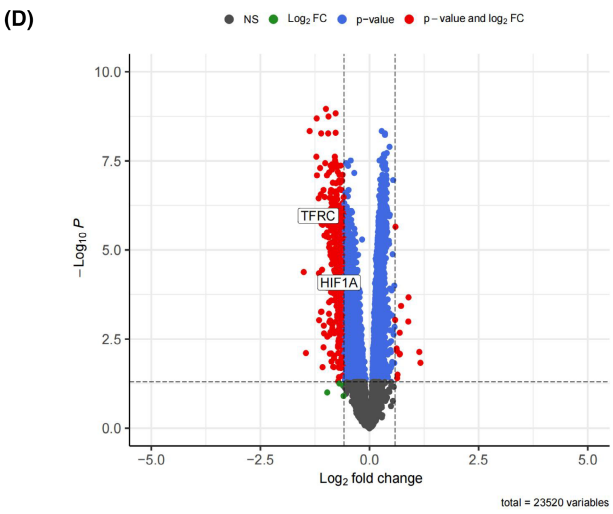

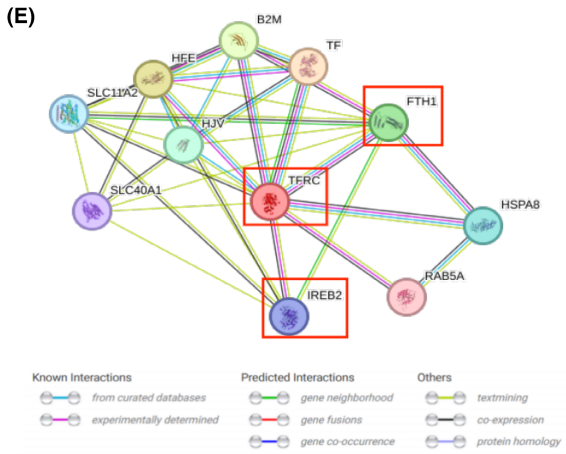

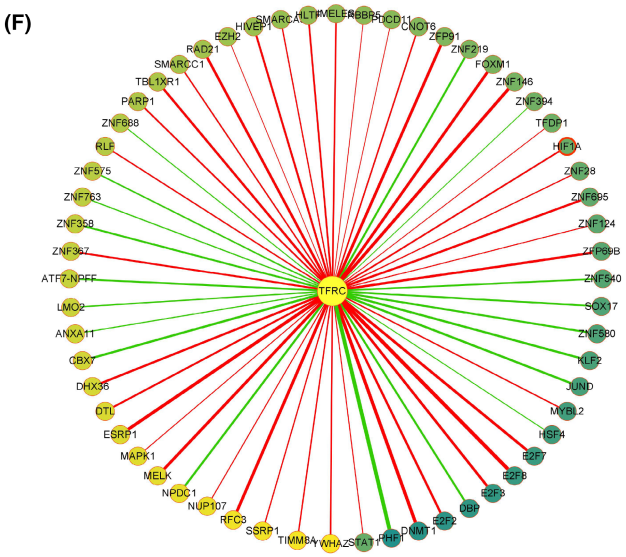

expression levels of TFRC, IREB2, FTH1, and HIF1α were significantly greater than those in the normal breast tissue samples ($p < .05$; Tables 1 and 2, Figure 2A–F). Similar results were observed for Western blotting and qRT-PCR analyses, and the differences between groups were significant ($p < .05$, Figure 2G–I).

TABLE 1 The average optical density of TFRC, IREB2, and FTH1 in breast cancer and normal breast tissues [$\bar{x} \pm s$].

	n	TFRC	IREB2	FTH1
Tumor	150	136.63 ± 15.64*	154.73 ± 16.22*	106.06 ± 11.03*
Normal	150	76.82 ± 4.65*	72.23 ± 5.36*	65.64 ± 6.77*

Abbreviations: FTH1, ferritin heavy chain 1; IREB2, iron-responsive element-binding protein 2; TFRC, transferrin receptor.

*$p < .05$.

TABLE 2 The expression of TFRC, IREB2, and FTH1 in breast cancer and normal breast tissues [*n* (%)].

	n	TFRC (+)	*p*	IREB2 (+)	*p*	FTH1 (+)	*p*
Tumor	150	96 (64)	.001*	102 (68)	.001*	133 (88.67)	.001*
Normal	150	59 (39.33)		53 (35.33)		22 (14.67)	

Abbreviations: FTH1, ferritin heavy chain 1; IREB2, iron-responsive element-binding protein 2; TFRC, transferrin receptor.

*$p < .05$.

The levels of Fe^{2+}, MDA, and GSH were measured using assay kits. The results showed that the average levels of Fe^{2+}, MDA, and GSH in breast cancer tissues were significantly greater than those in normal breast tissues ($p < .05$, Figure 2J). The levels of Fe^{2+}, MDA, and GSH were positively correlated with breast cancer ($p < .05$, Table 3).

3.3.2 | Expression of HIF1α, IREB2, TFRC, FTH1, and ferroptosis markers in TAC neoadjuvant treatment-sensitive and resistant groups of breast cancer

Immunohistochemical analysis was conducted on 97 cases of TAC neoadjuvant treatment-sensitive and 53 cases of treatment-resistant breast cancer samples to assess the expression of TFRC, IREB2, FTH1, and HIF1α. Compared with the average OD values, the percentages of TFRC- and HIF1α-positive cells were significantly lower in the resistant group than in the sensitive group ($p < .05$). However, the expression of IREB2 and FTH1 did not significantly differ between the two groups ($p > .05$, Tables 4 and 5, Figure 3A–H). Linear regression trend line analysis revealed a positive correlation between the expression of HIF1α and TFRC in the resistant group ($p < .05$); however, HIF1α expression was not correlated with IREB2 or FTH1 ($p > .05$, Figure 3I).

The results of Western blotting and qRT-PCR assays showed that the protein and mRNA levels of TFRC and HIF1α were significantly lower in the resistant group than in the sensitive group ($p < .05$). However, the differences in the protein and mRNA expression levels of IREB2 and FTH1 between the sensitive and resistant groups were not significant ($p > .05$, Figure 3J–L).

By measuring the levels of Fe^{2+}, MDA, and GSH in breast cancer-sensitive and resistant groups using their respective assay kits, we found that in the sensitive group, the average levels of Fe^{2+} and MDA were significantly greater than those in the resistant group ($p < .05$, Figure 3M). Although the GSH content was lower in the sensitive group than in the resistant group, the difference between the groups was not significant ($p > .05$).

3.3.3 | Correlation between tumor regression and expression of various factors in breast cancer

Using linear regression equations based on tumor regression grading criteria, we analyzed the correlations between HIF1α, IREB2, TFRC, FTH1, Fe^{2+}, MDA, and GSH, and tumor regression rates. The results showed a positive correlation between tumor regression and the expression of TFRC and HIF1α ($p < .05$); however, no correlation was found between the expression of IREB2 and FTH1 ($p > .05$, Figure 3N). The Fe^{2+} and MDA levels were positively correlated with tumor regression ($p < .05$, Figure 3O), whereas the correlation between GHS and tumor regression was not significant ($p > .05$). This finding suggested that the ADR-sensitive group of patients with breast cancer may have a greater risk of ferroptosis than the ADR-resistant group.

3.4 | Cell experiment validation of the effect of HIF1α, TFRC, and ferroptosis on the resistance of breast cancer to ADR

3.4.1 | Cell line screening and ADR-sensitivity testing

To assess the expression of HIF1α and its sensitivity to ADR in six cell lines, we evaluated the expression of HIF1α in each cell line. The results of Western blotting assays

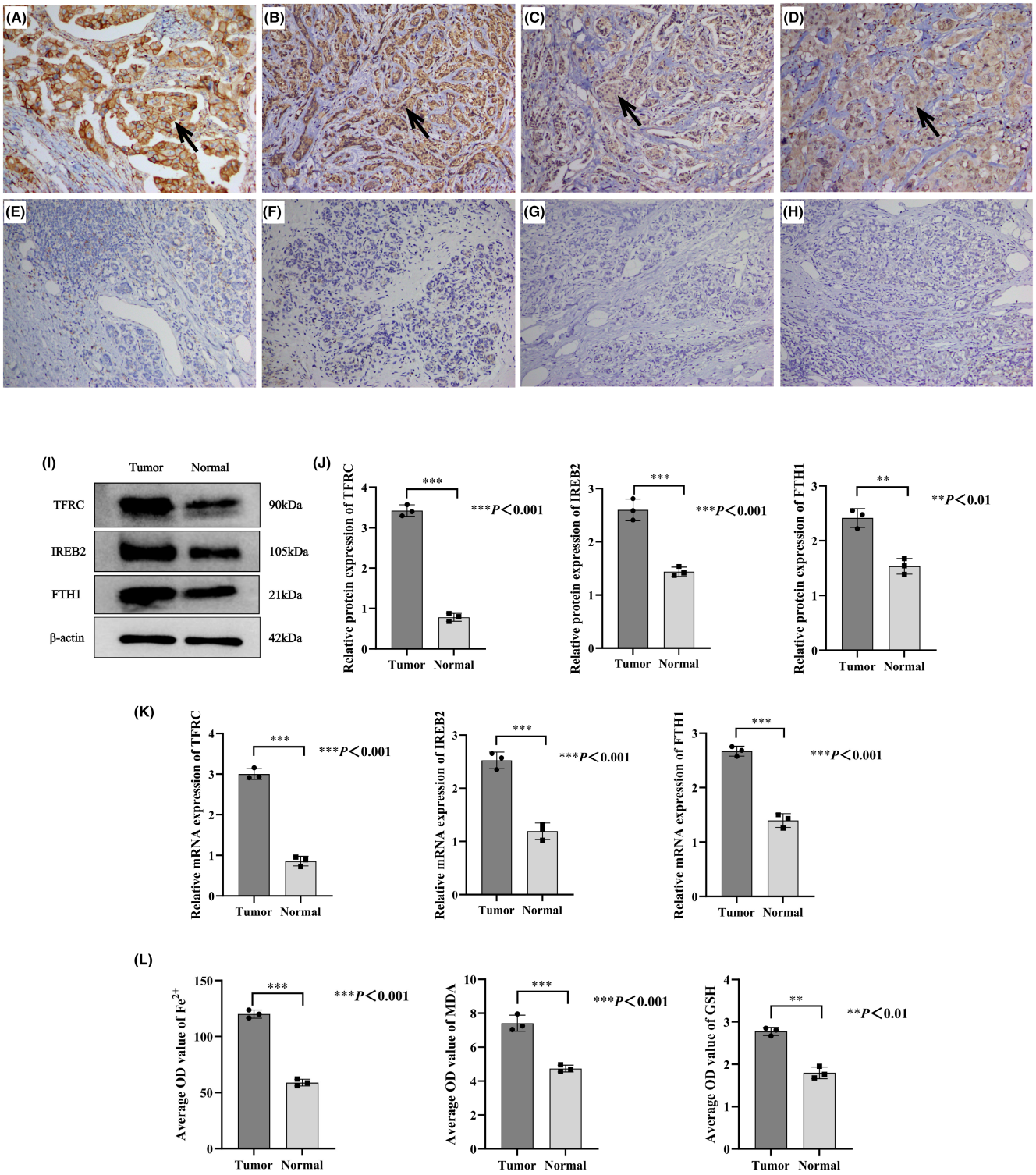

FIGURE 2 The differences in ferroptosis-related factors between breast cancer and normal breast tissue. (A–D) Transferrin receptor (TFRC), iron-responsive element-binding protein 2 (IREB2), ferritin heavy chain 1 (FTH1), and hypoxia-inducible factor-1α (HIF1α) shows positive expression in breast cancer. (E–H) TFRC, IREB2, FTH1, and HIF1α shows negative expression in normal breast tissue (Immunohistochemistry EnVision method, ×200, consecutive slices of the same tissue in the same field of view). (I and J) Protein expression of TFRC, IREB2, and FTH1 in breast cancer and normal breast tissue (Western blot electrophoretogram and Western blot histograms). (K) mRNA expression of TFRC, IREB2, and FTH1 in breast cancer and normal breast tissue (qRT-PCR histograms). (L) OD values of iron ion (Fe^{2+}), malondialdehyde (MDA), and glutathione (GSH) in breast cancer and normal breast tissue. The tissue samples were collected from 150 patients that were included in this study. Protein expression in tissue samples was detected using Western blot and mRNA expression in tissue samples was detected using RT-PCR. Fe^{2+}, MDA, and GSH in breast cancer and normal breast tissue were detected using respective detection kit. All experiments were performed in triplicate with at least three independent samples. $^{*}p < .05$, $^{**}P < .01$, $^{***}P < .001$ are statistically significant.

TABLE 3 Correlation of Fe^{2+}, MDA, and GSH expression with breast cancer as well as normal breast tissue.

		Fe^{2+}				MDA				GSH			
	n	+	−	*r*	*p*	+	−	*r*	*p*	+	−	*r*	*p*
Tumor	70	59	11	0.545	.001*	57	13	0.559	.001*	49	21	0.357	.001*
Normal	70	21	48			18	52			24	46		

Abbreviations: Fe^{2+}, iron ion; GSH, glutathione; MDA, malondialdehyde.

*$p < .05$.

TABLE 4 The average optical density of TFRC, IREB2, FTH1, and HIF1α in breast cancer and normal breast tissues [$\bar{x} \pm s$].

	n	TFRC	IREB2	FTH1	HIF1α
Sensitive	97	163.67 ± 25.32*	166.39 ± 25.76	76.06 ± 9.03	171.34 ± 24.62*
Drug-resistant	53	90.65 ± 15.31*	167.43 ± 16.26	74.61 ± 14.34	89.61 ± 14.27*

Abbreviations: FTH1, ferritin heavy chain 1; HIF1α, hypoxia-inducible factor-1α; IREB2, iron-responsive element-binding protein 2; TFRC, transferrin receptor.

*$p < .05$.

TABLE 5 The expression of TFRC, IREB2, FTH1, and HIF1α in the sensitive and resistant groups of breast cancer [*n* (%)].

	n	TFRC (+)	IREB2 (+)	FTH1 (+)	HIF1α
Sensitive	97	72 (74.23)	78 (80.41)	5 (5.15)	74 (76.29)
Drug-resistant	53	20 (37.74)	24 (45.28)	17 (32.08)	22 (41.51)

Abbreviations: FTH1, ferritin heavy chain 1; HIF1α, hypoxia-inducible factor-1α; IREB2, iron-responsive element-binding protein 2; TFRC, transferrin receptor.

showed that the expression of HIF1α was the highest in the MCF-7 cells and lowest in the BT-549 cells ($p < .05$, Figure 4A). The results of the CCK-8 assay showed that the IC50 of BT-549 cells was significantly higher than that of the other groups of cells, with IC50 values of 57.62 μmol/L for BT-549, 32.80 μmol/L for BT-20, 25.46 μmol/L for BT-474, 21.42 μmol/L for HCC1954, 19.42 μmol/L for MDA-MB-435, and 5.64 μmol/L for MCF-7 ($p < .05$, Figure 4B). The IC50 of BT-549 cells was 10.22 times higher than that of the MCF-7 cells, indicating resistance to ADR. Thus, we selected MCF-7 cells, with high expression of HIF1α and highly sensitive to ADR, and BT-549 cells, with low expression of HIF1α and resistant to ADR, for subsequent experiments.

3.4.2 | Expression of HIF1α, IREB2, TFRC, FTH1, and ferroptosis-related factors in MCF-7 and BT-549 cells

The results of Western blotting and qRT-PCR assays showed that the expression of HIF1α and TFRC in MCF-7 cells was significantly greater than that in BT-549 cells ($p < .05$, Figure 4C). However, the difference in

FIGURE 3 Differences in ferroptosis-related factors between the sensitive and resistant groups in breast cancer TAC treatment. (A) Transferrin receptor (TFRC) shows positive expression in the sensitive group. (B) Iron-responsive element-binding protein 2 (IREB2) exhibits positive expression in the sensitive group. (C) Ferritin heavy chain 1 (FTH1) demonstrates negative expression in the sensitive group. (D) Hypoxia-inducible factor-1α (HIF1α) displays positive expression in the sensitive group. (E) TFRC shows weak positive expression in the resistant group. (F) IREB2 exhibits positive expression in the resistant group. (G) FTH1 demonstrates negative expression in the resistant group. (H) HIF1α displays weak positive expression in the resistant group (Immunohistochemistry EnVision method, ×200, consecutive slices of the same tissue in the same field of view). (I) In breast cancer, the correlation between HIF1α and the expression of TFRC, IREB2, and FTH1. (J–L) mRNA and protein expression of TFRC, IREB2, FTH1, and HIF1α in the sensitive and resistant groups of breast cancer TAC treatment (qRT-PCR histograms, Western blot electrophoresis, and Western blot histograms). (M) OD values of iron ion (Fe^{2+}), malondialdehyde (MDA), and glutathione (GSH) in the sensitive and resistant groups of breast cancer TAC treatment. (N) Correlation between tumor regression rate and the expression of TFRC, IREB2, FTH1, and HIF1α. (O) Correlation between tumor regression rate and the expression of Fe^{2+}, MDA, and GSH. The tissue samples were collected from 150 patients that were included in this study. Protein expression in tissue samples was detected using Western blot and mRNA expression in tissue samples was detected using RT-PCR. Fe^{2+}, MDA, and GSH in breast cancer were detected using respective detection kit. All experiments were performed in triplicate with at least three independent samples. *$p < .05$, **$P < .01$, ***$P < .001$ are statistically significant.

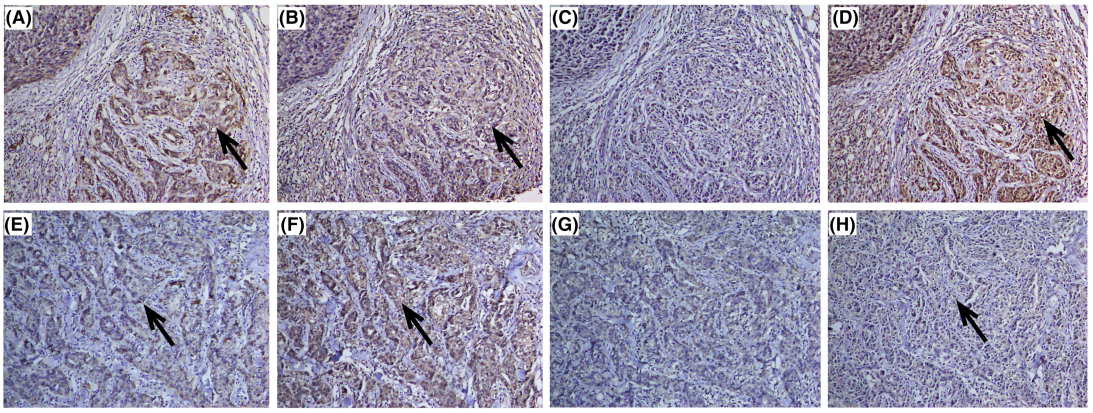
(A)
(B)
(C)
(D)
(E)
(F)
(G)
(H)

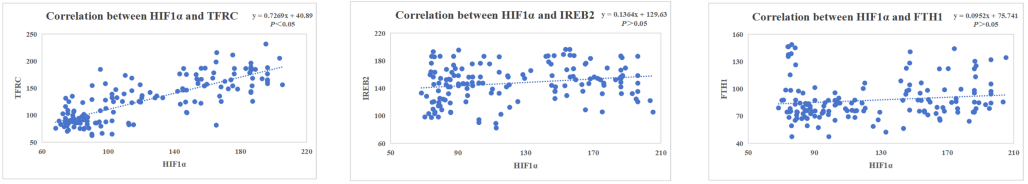
(I)
Correlation between HIF1α and TFRC
Correlation between HIF1α and IREB2
Correlation between HIF1α and FTH1
HIF1α
TFRC
IREB2
FTH1

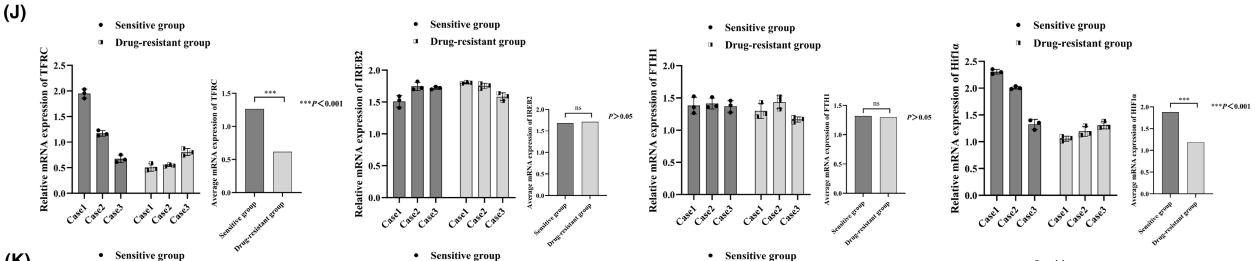
(J)
Sensitive group
Drug-resistant group
Relative mRNA expression of TFRC
Relative mRNA expression of IREB2
Relative mRNA expression of FTH1
Relative mRNA expression of Hif1α
***P<0.001
P>0.05

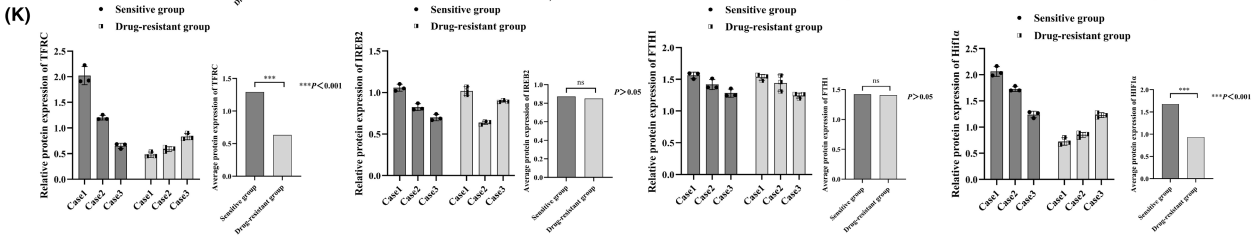
(K)
Sensitive group
Drug-resistant group
Relative protein expression of TFRC
Relative protein expression of IREB2
Relative protein expression of FTH1
Relative protein expression of Hif1α
***P<0.001
P>0.05

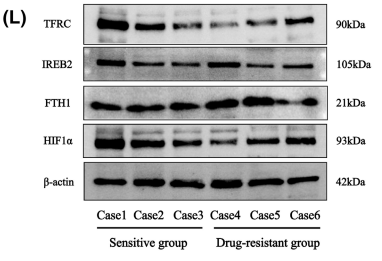
(L)
TFRC
IREB2
FTH1
HIF1α
β-actin
90kDa
105kDa
21kDa
93kDa
42kDa
Case1 Case2 Case3 Case4 Case5 Case6
Sensitive group
Drug-resistant group

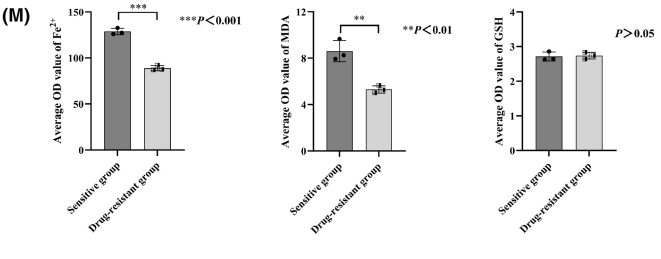
(M)
Average OD value of Fe2+
Average OD value of MDA
Average OD value of GSH
***P<0.001
**P<0.01
P>0.05
Sensitive group
Drug-resistant group

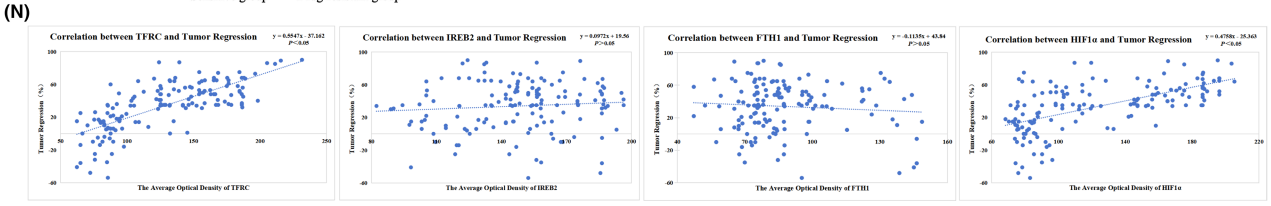
(N)
Correlation between TFRC and Tumor Regression
Correlation between IREB2 and Tumor Regression
Correlation between FTH1 and Tumor Regression
Correlation between HIF1α and Tumor Regression
Tumor Regression (%)
The Average Optical Density of TFRC
The Average Optical Density of IREB2
The Average Optical Density of FTH1
The Average Optical Density of HIF1α

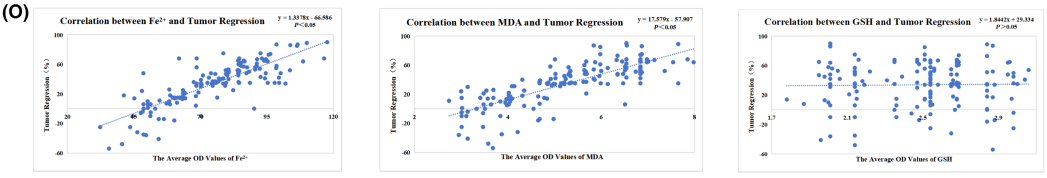
(O)
Correlation between Fe2+ and Tumor Regression
Correlation between MDA and Tumor Regression
Correlation between GSH and Tumor Regression
Tumor Regression (%)
The Average OD Values of Fe2+
The Average OD Values of MDA
The Average OD Values of GSH

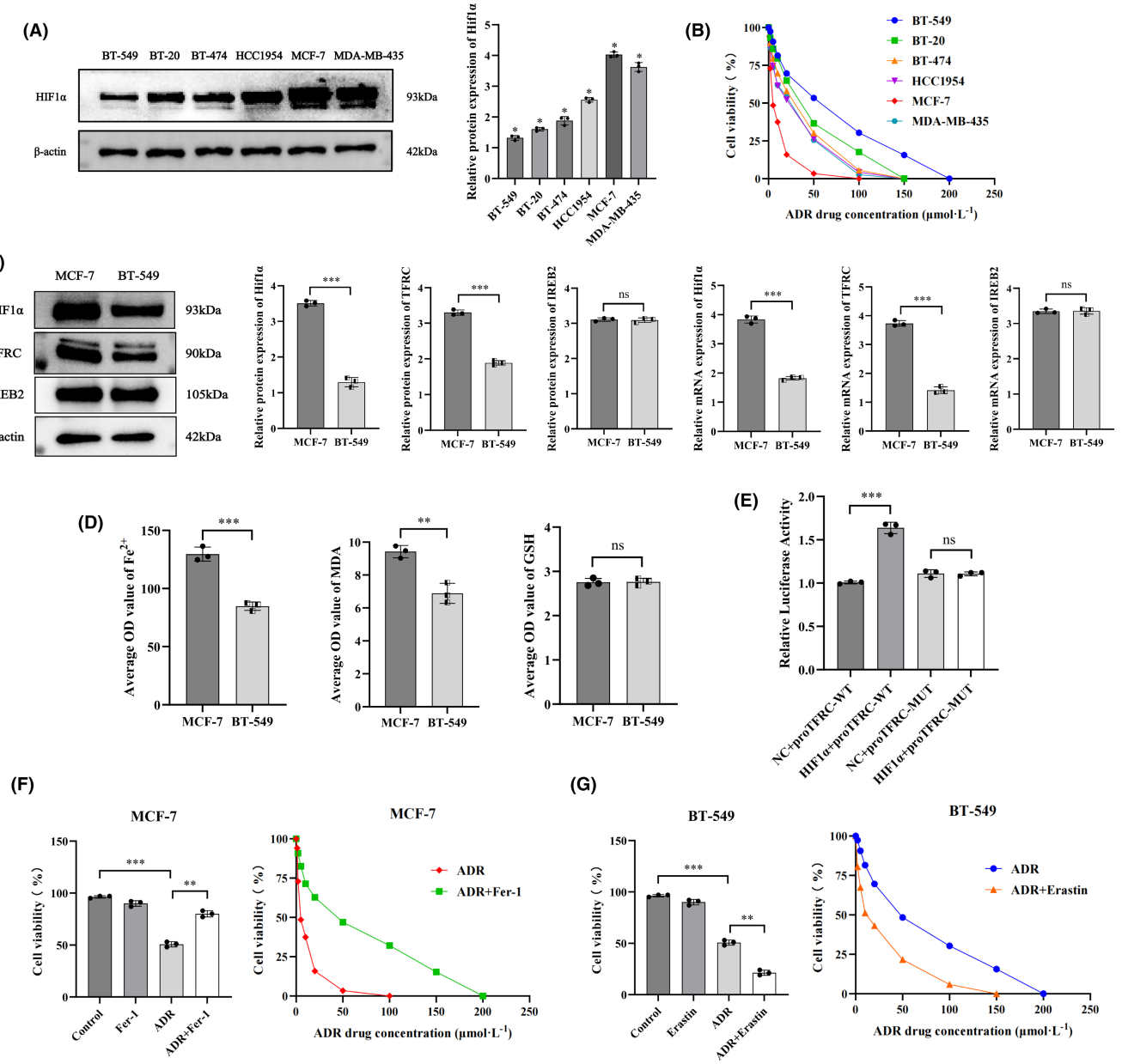

FIGURE 4 Cell experiments validate the effects of Hypoxia-inducible factor-1α (HIF1α), transferrin receptor (TFRC), and ferroptosis on Adriamycin (ADR) resistance in breast cancer. (A) The expression levels of HIF1α in six cell lines. (B) The chemical sensitivity of six cell lines to ADR (dose–response curve). (C) The protein and mRNA expression levels of HIF1α, TFRC, and iron-responsive element-binding protein 2 (IREB2) in MCF-7 and BT-549 cells (Western blot electrophoresis, Western blot histograms, and qRT-PCR histograms). (D) The optical density (OD) values of iron ion (Fe^{2+}), malondialdehyde (MDA), and glutathione (GSH) in MCF-7 and BT-549 cells. (E) Double luciferase assay confirmed the direct binding of HIF1α to TFRC. (F) Cell viability and chemosensitivity to ADR (dose–response curve) in each group of MCF-7 cells. (G) Cell viability and chemosensitivity to ADR (dose–response curve) in each group of BT-549 cells. Cells were incubated with culture medium containing different concentrations of ADR drugs for 24 h before cell counting kit-8 (CCK-8) assay was performed. All experiments were performed in triplicate with at least three independent samples. *$p < .05$, **$P < .01$, ***$P < .001$ are statistically significant.

the expression of IREB2 between the two cell lines was not significant ($p > .05$). We also found that the levels of Fe^{2+} and MDA in MCF-7 cells were significantly greater than those in BT-549 cells ($p < .05$, Figure 4D), whereas the difference in GSH levels between the two cell lines was not significant ($p > .05$). These results suggested that sensitive breast cancer cells exhibit a greater iron state than resistant cells, thus increasing the risk of ferroptosis induction, which is associated with the abundance of HIF1α and TFRC.

3.4.3 | Experimental study on the effect of ferroptosis on the sensitivity of breast cancer cells to ADR

To validate the association between the sensitivity of breast cancer cells to ADR and ferroptosis, we conducted rescue experiments using the ferroptosis inhibitor Fer-1 and the ferroptosis activator Erastin along with ADR treatment. The results of the CCK-8 assay showed that for the MCF-7 cells, the cell survival rate in the ADR group was significantly lower than that in the ADR + Fer-1, Fer-1, and saline groups ($p < .05$). However, the cell survival rate in the ADR + Fer-1 group was greater than that in the ADR group but lower than that in the saline and Fer-1 groups. The IC50 value of the ADR + Fer-1 group was significantly greater than that of the ADR group ($p < .05$, Figure 4F). For BT-549 cells, the cell survival rate in the ADR + Erastin group was significantly lower than that in the other three groups. The IC50 value of the ADR + Erastin group was significantly lower than that of the ADR group ($p < .05$, Figure 4G). These results suggested that the sensitivity of breast cancer cells to ADR is related to ferroptosis, and activating ferroptosis can significantly increase the sensitivity of breast cancer cells to ADR.

3.4.4 | Dual-luciferase assay was performed to validate the interaction between HIF1α and TFRC

To assess the direct interaction between HIF1α and TFRC, we conducted a dual-luciferase assay. Compared to those in the control group, a significant difference in the binding efficacy between the DNA of HIF1α and the protein of TFRC was detected, with a significant increase in fluorescence intensity ($p < .05$, Figure 4E). This suggested that HIF1α can act as a transcription factor for TFRC, initiating its transcription and affecting its expression.

3.4.5 | Regulatory effects of HIF1α on TFRC and ferroptosis-related factors in breast cancer cell lines

Initially, MCF-7 cells were transfected with lentivirus carrying specific sh-HIF1α sequences, while BT-549 cells were transfected with lentivirus carrying OE-HIF1α sequences. The results of Western blotting analysis showed that in the MCF-7 cells, the expression of HIF1α decreased significantly in the sh-HIF1α group compared to that in the sh-NC and control groups. In contrast, in the BT-549 cells, the level of HIF1α expression was significantly greater in the OE-HIF1α group than in the other two groups, demonstrating successful transfection ($p < .05$; Figure 5A,B). The results of subsequent Western blotting and qRT-PCR analyses showed that in MCF-7 cells, the protein and mRNA expression levels of TFRC were significantly lower in the sh-HIF1α group than in the control and sh-NC groups. In contrast, in the BT-549 cells, the protein and mRNA expression levels of TFRC were significantly greater in the OE-HIF1α group than in the control and sh-NC groups ($p < .05$, Figure 5A,B). The difference between the sh-NC and control groups was not significant ($p > .05$).

The levels of Fe^{2+}, MDA, and GSH were determined in MCF-7 and BT-549 cells after transfection with HIF1α using suitable assay kits. The results showed that the levels of Fe^{2+} and MDA in the sh-HIF1α group of MCF-7 cells were lower than those in the control and sh-NC groups (Table 6). In contrast, for BT-549 cells, the levels of Fe^{2+} and MDA were significantly greater in the OE-HIF1α group than those in the other groups ($p < .05$, Table 7); however, the difference in GSH levels between the groups was not significant ($p > .05$). FerroOrange fluorescence staining showed that the average light density of Fe^{2+} fluorescence in the sh-HIF1α group of MCF-7 cells was significantly lower, while in the OE-HIF1α group of BT-549 cells, the average light density of Fe^{2+} fluorescence was significantly greater ($p < .05$, Figure 5C).

The experimental results suggested that HIF1α can regulate the expression of TFRC, thus affecting the concentration of Fe^{2+} and, consequently, influencing ferroptosis associated with breast cancer resistance.

3.4.6 | Effect of HIF1α regulation on ADR sensitivity in breast cancer MCF-7 and BT-549 cells

To determine the regulatory effect of HIF1α on ADR sensitivity in breast cancer cells, we conducted CCK-8 experiments and assessed cell viability before and after transfection of MCF-7 and BT-549 cells with HIF1α combined with ADR. Compared to those in the control group and the sh-NC group, the percentage of surviving MCF-7 cells in the sh-HIF1α group increased significantly, while the percentage of surviving BT-549 cells in the OE-HIF1α group decreased significantly when the cells were exposed to the same drug concentration ($p < .05$; Tables 8 and 9).

Further examination of the regulatory effect of HIF1α on the ADR IC50 values of each group of cells showed that the IC50 values of ADR in MCF-7 cells were 5.64 ± 0.13, 5.61 ± 0.21, and $41.7 \pm 4.2\,\mu mol/L$ for the control group, sh-NC group, and sh-HIF1α group, respectively. In BT-549 cells, the IC50 values of ADR were 57.54 ± 3.65, 57.48 ± 3.58, and $8.05 \pm 1.43\,\mu mol/L$ for the control group,

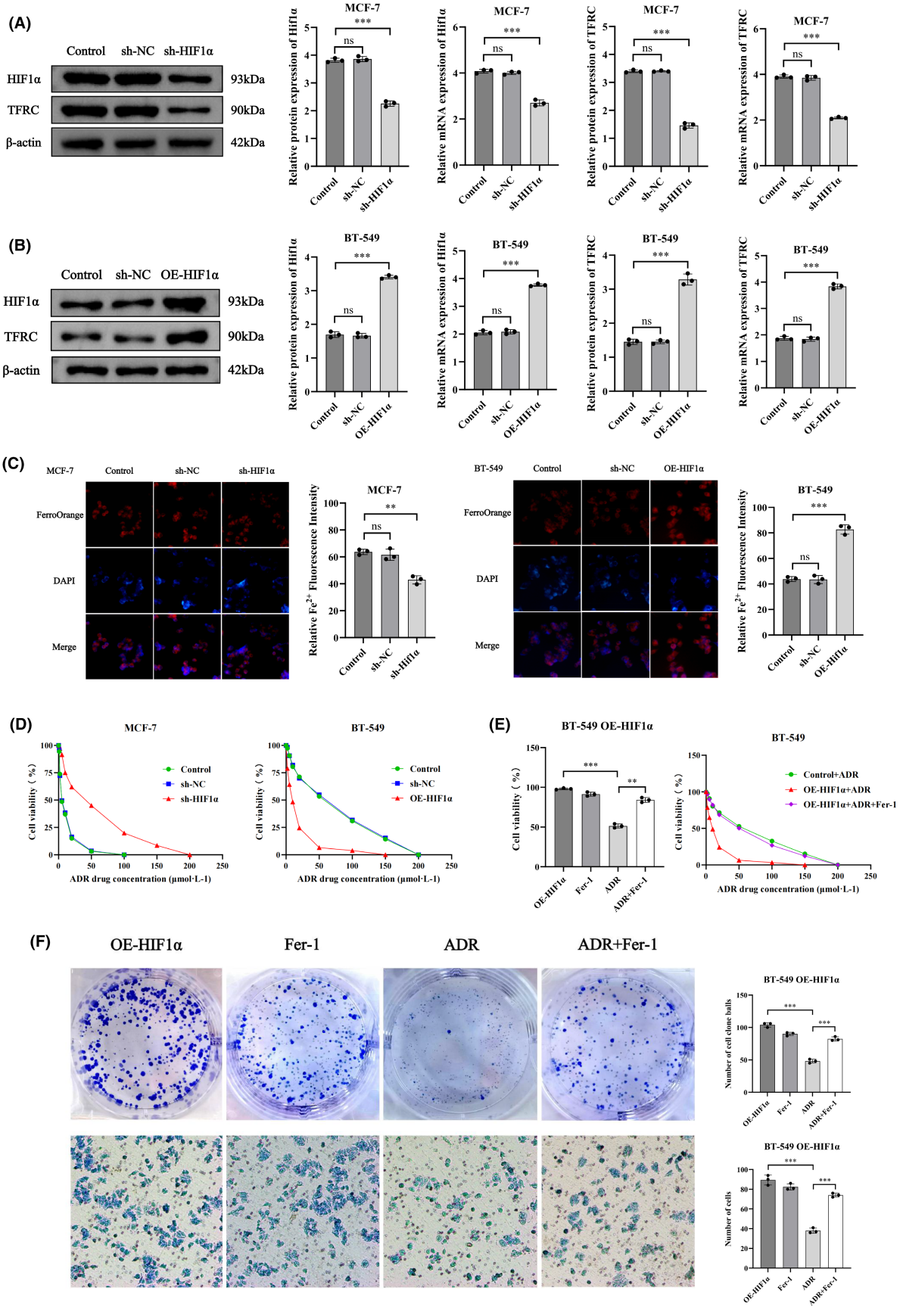
(A)
Control
sh-NC
sh-HIF1α
HIF1α
TFRC
β-actin
93kDa
90kDa
42kDa
MCF-7
Relative protein expression of Hif1α
Relative mRNA expression of Hif1α
Relative protein expression of TFRC
Relative mRNA expression of TFRC
(B)
OE-HIF1α
BT-549
(C)
FerroOrange
DAPI
Merge
Relative Fe2+ Fluorescence Intensity
(D)
Cell viability (%)
ADR drug concentration (μmol·L-1)
(E)
BT-549 OE-HIF1α
Control+ADR
OE-HIF1α+ADR
OE-HIF1α+ADR+Fer-1
(F)
OE-HIF1α
Fer-1
ADR
ADR+Fer-1
Number of cell clone balls
Number of cells

FIGURE 5 The regulatory effect of hypoxia-inducible factor-1α (HIF1α) on the multidrug resistance of breast cancer cells. (A) Twenty-four hours after transfection with sh-HIF1α sequences, the protein and mRNA expression levels of HIF1α and transferrin receptor (TFRC) in MCF-7 cells for each group. (B) Twenty-four hours after transfection with OE-HIF1α sequences, the protein and mRNA expression levels of HIF1α and transferrin receptor (TFRC) in BT-549 cells for each group. (C) After lentiviral transduction, MCF-7 and BT-549 cells were subjected to FerroOrange fluorescence staining in their respective groups (fluorescent staining and relative iron ion (Fe^{2+}) fluorescence intensity). (D) After lentiviral transduction, the chemical sensitivity of MCF-7 and BT-549 cells to Adriamycin (ADR) (dose–response curve). (E) Cell viability and chemosensitivity to adverse reactions to ADR (dose–response curve) in each group of BT-549 cells after upregulation of HIF1α combined with Fer-1. (F) Plate clone assay and Transwell assay of BT-549 cells in each group after upregulation of HIF1α combined with Fer-1. Cells were incubated with culture medium containing different concentrations of ADR drugs for 24 h before cell counting kit-8 (CCK-8) assay was performed. Cells were cultured with a medium for 1 week for the colonies were counted. All experiments were performed in triplicate with at least three independent samples. *$p < .05$, **$P < .01$, ***$P < .001$ are statistically significant.

TABLE 6 The average OD values of Fe^{2+}, MDA, and GSH in various groups of MCF-7 cell lines [$\bar{x} \pm s$].

	Fe^{2+}	MDA	GSH
Control	73.25 ± 5.85*	5.64 ± 0.54*	2.54 ± 0.34
Sh-NC	72.54 ± 5.67*	5.71 ± 0.23*	2.60 ± 0.23
sh-HIF1α	41.25 ± 4.51*	3.02 ± 0.31*	2.71 ± 0.31

Abbreviations: Fe^{2+}, iron ion; GSH, glutathione; MDA, malondialdehyde; OD, optical density.

*$p < .05$.

TABLE 7 The average OD values of Fe^{2+}, MDA, and GSH in various groups of BT-549 cell lines [$\bar{x} \pm s$].

	Fe^{2+}	MDA	GSH
Control	43.25 ± 4.85*	3.64 ± 0.54*	2.54 ± 0.34
Sh-NC	42.54 ± 4.67*	3.71 ± 0.23*	2.60 ± 0.23
OE-HIF1α	85.26 ± 6.84*	5.24 ± 1.21*	2.56 ± 0.32

Abbreviations: Fe^{2+}, iron ion; GSH, glutathione; HIF1α, hypoxia-inducible factor-1α; MDA, malondialdehyde; OD, optical density.

*$p < .05$.

TABLE 8 Average survival rate of cell lines in MCF-7 groups [$\bar{x} \pm s$] (%).

	Control	sh-NC	sh-HIF1α
Before applying ADR	97.32 ± 2.31*	96.43 ± 2.27*	97.68 ± 2.30*
After applying ADR	51.18 ± 3.24*	50.84 ± 3.41*	66.31 ± 5.68*

Abbreviations: ADR, Adriamycin; HIF1α, hypoxia-inducible factor-1α.

*$p < .05$.

TABLE 9 Average survival rate of cell lines in BT-549 groups [$\bar{x} \pm s$] (%).

	Control	sh-NC	OE-HIF1α
Before applying ADR	98.13 ± 1.23*	97.58 ± 2.65*	93.65 ± 3.39*
After applying ADR	49.35 ± 3.86*	50.65 ± 3.15*	28.61 ± 2.84*

Abbreviations: ADR, Adriamycin; HIF1α, hypoxia-inducible factor-1α.

*$p < .05$.

sh-NC group, and OE-HIF1α group, respectively. The IC50 value of ADR in the BT-549 OE-HIF1α group was significantly lower than that in the control group and the sh-NC group, while in MCF-7 cells, the IC50 value of ADR increased significantly in the sh-HIF1α group after HIF1α was downregulated ($p < .05$, Figure 5D).

These results suggested that upregulation of HIF1α induces the overexpression of TFRC to induce ferroptosis, which significantly increases the sensitivity of breast cancer cells to ADR and reverses their resistance.

3.4.7 | Ferroptosis inhibitor can rescue HIF1α-upregulated BT-549 cells from ADR cytotoxicity

To determine the association between ferroptosis and the sensitivity of HIF1α-upregulated BT-549 cells to ADR, we conducted rescue experiments using the ferroptosis inhibitor Fer-1. The results of the CCK-8 assay showed that at the same drug concentration, the viability of the OE-HIF1α BT-549 cells in the ADR group was significantly lower than that in the other three groups ($p < .05$). However, the cell viability of the ADR + Fer-1 group was significantly greater than that of the ADR group but lower than the cell viability in the physiological saline group and Fer-1 group. The IC50 value of the ADR + Fer-1 group (50.97 ± 3.83 μmol/L) was significantly greater than that of the ADR group ($p < .05$, Figure 5E), and it was similar to the IC50 value of the control group.

These results indicated that the ferroptosis inhibitor Fer-1 can rescue the cytotoxic effect of ADR on HIF1α-upregulated breast cancer-resistant cells. This finding confirmed that upregulation of HIF1α can activate ferroptosis in resistant breast cancer cells, thus significantly increasing their sensitivity to ADR and reversing their resistance.

3.4.8 | Effect of the upregulation of HIF1α combined with ADR on the biological behavior of BT-549 cells

To determine the role of ferroptosis activation in the inhibition of the biological behavior of BT-549 cells after the upregulation of HIF1α, colony formation, and Transwell assays were conducted, and the proliferation and invasion abilities of cells in each group were evaluated. The results showed that when applying an equal dosage of ADR (57.62 μmol/L; selected based on the preexperiment IC50 value of BT-549 cells), the proliferation and invasion abilities of cells in the ADR group of OE-HIF1α BT-549 cells were significantly lower than those in the other three groups ($p < .05$). Additionally, the proliferation and invasion abilities of cells in the ADR + Fer-1 group were significantly greater than those in the ADR group ($p < .05$, Figure 5F).

These findings confirmed that upregulation of HIF1α can activate ferroptosis in resistant breast cancer cells, thus significantly enhancing their sensitivity to ADR and reversing their resistance.

4 | DISCUSSION

Resistance of tumor cells to chemotherapeutic drugs is a major problem in clinical practice that needs to be solved. Breast cancer is one of the most common malignant tumors in women and is resistant to doxorubicin (ADR) in clinical treatment, which is a crucial factor affecting patient prognosis. The mechanisms underlying tumor resistance are complex, and comprehensive research on the causes and mechanisms of ADR resistance in breast cancer is necessary for reversing ADR resistance in breast cancer and improving patient prognosis.

Therefore, in this study, we initially selected three pairs of breast cancer samples treated with the TAC neoadjuvant chemotherapeutic regimen. By conducting differential analysis, we identified 27 differentially expressed genes (DEGs). The KEGG pathway enrichment analysis showed that among these DEGs, the TFRC was enriched in the ferroptosis pathway; the level of expression of the TFRC mRNA in breast cancer-resistant cases was low. The TFRC protein is an essential intracellular iron transporter that mediates the uptake of extracellular iron ions. Thus, it plays a crucial role in maintaining cellular iron metabolism and serves as a key molecule involved in initiating ferroptosis.[6–8] Some researchers have found that TFRC plays a key role in ferroptosis. Several studies have shown that iron ions are necessary for the growth and metabolism of cells, particularly tumor cells, where high iron levels can meet the demands of high metabolism and unlimited proliferation.[9] In a study, Pinnix et al. reported that breast cancer cells exhibit greater uptake and lower efflux of iron ions, which results in greater labile iron pools in breast cancer tissues than in normal tissues.[10] Wang et al. reported that iron ion levels in breast cancer tissues are greater than those in normal breast tissues, and this increase is associated with the upregulation of TFRC.[11] However, in this study, the preliminary experiments and the bioinformatics analysis conducted showed that TFRC expression in breast cancer was heterogeneous, with low levels of expression in resistant cells accompanied by low iron ion levels; in contrast, in sensitive cells, TFRC was expressed at high levels along with higher iron ion levels.[12] Therefore, we hypothesized that breast cancer cells in the ADR-sensitive group, characterized by high TFRC expression and iron ion levels, have a greater risk of ferroptosis than cells in the ADR-resistant group. These cells are more prone to ferroptosis activation through the Fenton reaction initiated by the association between high iron and H_2O_2 produced by AD.[13–15] In contrast, the ADR-resistant group exhibited low TFRC and Fe^{2+} expression, decreasing susceptibility to ferroptosis and thus leading to ADR resistance. Therefore, further insights into the regulatory mechanisms underlying differential TFRC expression and ferroptosis activation may greatly help determine the mechanism of ADR resistance.

To identify the factors influencing TFRC expression, we conducted further analyses using bioinformatics techniques. First, we analyzed the significance of the difference in the expression of the TFRC gene using the GEPIA and UALCAN databases. The results indicated a close relationship between the TFRC gene and tumors, with significant differences in the expression of TFRC observed across 33 types of cancers, including breast cancer, where the expression of TFRC was greater in tumor tissues than in normal breast tissues. Furthermore, analysis of the differential gene distribution in the whole transcriptome spectrum using the GEO database showed that TFRC mRNA was significantly downregulated in chemotherapy-resistant patients treated with ADR, which was consistent with our transcriptomic sequencing results. Next, we constructed a TFRC protein interaction network using the STRING database and found that IREB2 inhibits the degradation of the TFRC mRNA, while FTH1 is associated with ferroptosis-related proteins. Additionally, based on the TCGA database analysis, we predicted that the transcription factor HIF1α is a positive regulator influencing the transcription of the TFRC gene. Moreover, the GEO database analysis showed that HIF1α was significantly downregulated in ADR-resistant cases. The results of the bioinformatics analysis suggested a close association between breast cancer ADR resistance and low levels of expression of HIF1α and TFRC, leading to ferroptosis. Therefore, in this study, we investigated the mechanism by which HIF1α regulates TFRC and subsequently

affects ferroptosis and resistance of breast cancer to ADR. Through clinical sample validation and assessment of the underlying cellular mechanism, we identified the role of HIF1α in regulating TFRC and identified new ways to reverse drug resistance.

In ferroptosis, iron-dependent accumulation of lipid reactive oxygen species leads to cell death.[16] Its regulatory mechanisms and biochemical and morphological characteristics differ from those of other forms of cell death, such as apoptosis, necrosis, and autophagy. Among the various mechanisms involved in ferroptosis, the antioxidant system Xc-/GPX4 pathway and the TFRC iron transport pathway, which regulate iron metabolism, play important roles.[17] Researchers have found a close relationship between the GSH-GPX4 antioxidant enzyme system and ferroptosis. However, studies on the regulation of ferroptosis mediated by iron transport pathways are scarce. The iron transport protein pathway regulates the homeostasis of free iron ions in cells. Iron uptake mediated by TFRC and iron storage represented by the iron-binding protein FTH1, as well as iron efflux mediated by the solute carrier protein SLC40A1, constitute the balance system of intracellular iron ions. As the sole pathway for cellular iron intake, TFRC is not only an important factor in maintaining cellular iron metabolism but also the initiating factor for ferroptosis.[6] Therefore, regulating TFRC to maintain intracellular iron homeostasis is an important self-regulatory mechanism for cells. IREB2 is an RNA-binding protein that plays a key role in regulating iron. Studies have shown that IREB2 regulates the stability of the iron pool by sensing the concentration of iron ions. When intracellular iron ion concentration is low, IREB2 binds to the iron-responsive element (IRES) in the 3'-UTR of the TFRC mRNA, inhibiting the degradation of TFRC mRNA, thus increasing the expression of TFRC, promoting iron ion absorption, and increasing the abundance of iron ions. Additionally, IREB2 binds to the IRES in the 5'-UTR of ferritin mRNA (FTH1 mRNA), suppressing the translation of the FTH1 mRNA. This interaction decreases the binding of FTH1 to iron ions, ensuring that free iron ions are abundant and easily available.[11,18] With an increase in the understanding of the regulatory mechanisms of ferroptosis, the roles of IREB2 and TFRC (regulated by IREB2) in tumors have attracted attention. For example, Zhou et al. found that inhibiting the regulation of IREB2 in cellular iron metabolism can inhibit the proliferation of liver cancer cells.[19] Xia et al. studied COPD and found that N6-methyladenosine-modified circSAV1 promotes the translation of IREB2 by recruiting YTHDF1, triggering ferroptosis in COPD.[20] Lu et al. reported that neuroblastoma harboring MYCN amplification is prone to TFRC upregulation-induced ferroptosis.[21] Bioinformatics analysis revealed a coexpression relationship between TFRC and IREB2 and between TFRC and FTH1 in breast adenocarcinoma. To validate the results of this bioinformatics analysis, we initially conducted clinical sample research. The results showed that the positive expression rates of TFRC, IREB2, and FTH1 were higher in 150 cases of breast cancer tissues compared to their corresponding rates of expression in normal breast tissues, accompanied by an increase in the levels of Fe^{2+}, MDA, and GSH. We attributed this to the high rates of proliferation and metabolism in breast cancer cells. To meet their high iron metabolic demands, IREB2 is upregulated to regulate the high expression of TFRC, increase iron ion intake, and control the downregulation of FTH1, which decreases its ability to bind free iron ions, further increasing the abundance of intracellular iron ions to meet the high iron metabolic demands of breast cancer cells. However, the expression of TFRC, IREB2, and FTH1 in breast cancer was highly heterogeneous, and their relationship with the resistance of breast cancer to ADR remains unclear.

To elucidate the relationships among TFRC, IREB2, FTH1, and ADR resistance in breast cancer, we divided breast cancer patients into ADR-sensitive and ADR-resistant groups based on tumor regression grading criteria. IREB2 was highly expressed in the ADR-sensitive and ADR-resistant groups but was not associated with tumor regression. FTH1 exhibited a regulatory effect on IREB2. However, significant heterogeneity in the expression of the TFRC mRNA and protein was detected. TFRC expression was greater in the sensitive group than in the resistant group, accompanied by an increase in Fe^{2+}, which matched the regulatory effect of IREB2. In contrast, in the resistant group, TFRC was downregulated, accompanied by a decrease in Fe^{2+} and a positive correlation with tumor regression. In the resistant group, TFRC did not respond to the regulatory effect of IREB2, which indicated that IREB2 is not the sole factor affecting the expression of TFRC. We speculated that other factors may simultaneously influence the transcription or translation of TFRC in the resistant group, leading to the inhibition of TFRC expression, reducing iron ion intake, maintaining low iron homeostasis, and avoiding the risk of ferroptosis triggered by the Fenton reaction due to high iron levels and ADR. Additionally, we found no difference in the expression of GSH, suggesting that resistance of breast cancer to ADR may not be related to the endogenous GSH pathway. Our findings indicated that TFRC, Fe^{2+}, and resistance of breast cancer to ADR are related. Further information on the regulatory mechanisms that affect TFRC expression is important for inducing ferroptosis and reversing the resistance of breast cancer to ADR.

HIF1α can sense changes in oxygen levels in the cellular environment, particularly its response to hypoxia.[22,23] However, HIF1α not only regulates cellular adaptation to

hypoxia but also acts as a key transcription factor, facilitating the transcription of various downstream target genes, including platelet-derived growth factor, insulin-like growth factor, and vascular endothelial growth factor.[24–26] Specifically in the hypoxic tumor microenvironment, high expression of HIF1α promotes malignant tumor progression, leading to poor prognosis of patients.[27,28] It has also been found that HIF1α is an important pathway involved in the regulation of ferroptosis of a variety of cancerous cells and a number of molecules have been proposed to be regulated by HIF1α to activate ferroptosis.[29] In osteosarcoma cancer and glioma cells, SLC7A11 was found to mediate the regulatory effect of HIF1α on ferroptosis.[30,31] It has also been documented that HIF1α also enhances transcription of SLC1A1, an important glutamate transporter, and promotes cystine uptake to promote ferroptosis resistance in solid tumor cell.[32] Interestingly, some studies have found a correlation between HIF1α and TFRC expression in tumors. Chen et al. found that treating human osteosarcoma cell lines with HIF1α inducers can significantly upregulate the expression of TFRC.[33] Ozgü et al. showed that culturing brain microvascular endothelial cells under hypoxic conditions can induce stable expression of HIF1α, which increases the level of TFRC mRNA.[34] Pan et al. found that HIF1α can promote an increase in TFRC expression in heart tissues after heart failure.[35] HIF1α acts as a transcription factor that positively regulates TFRC expression and affects iron ion metabolism. We used bioinformatics databases to predict the transcription factor of TFRC and identified HIF1α as an upstream regulator of TFRC in breast cancer; thus, HIF1α has a positive regulatory effect on TFRC. Based on this finding, we hypothesized that the difference in the expression of TFRC between ADR-sensitive and resistant cases in breast cancer TAC neoadjuvant chemotherapy might be attributed to differences in the upstream transcription factor HIF1α. Clinical and cellular experiments were conducted to test this hypothesis. The results of clinical sample analysis showed that the level of expression of HIF1α and TFRC was lower in the ADR-resistant group of breast cancer compared to that in the ADR-sensitive group and showed a positive correlation, whereas the expression of IREB2 remained unchanged. To confirm these relationships, cell experiments were formed using MCF-7 cells with high HIF1α expression and sensitivity to ADR, as well as, BT-549 cells with low HIF1α expression and resistance to ADR. Consistent with the clinical sample results, we found that compared with resistant cells, breast cancer-sensitive cells exhibited a greater iron state, which correlated with the abundance of HIF1α and TFRC and posed a greater risk of ferroptosis induction. To verify that high iron ion concentrations mediated by HIF1α and TFRC can activate ferroptosis and thus influence the sensitivity of breast cancer cells to ADR, we conducted experiments in which ADR was combined with ferroptosis inhibitors and activators. The results showed that in ADR-sensitive cell lines, the combination of ADR and the ferroptosis inhibitor Fer-1 rescued tumor suppression caused by ADR, while in ADR-resistant cell lines, the combination of ADR with the ferroptosis activator reversed the resistance of tumor cells to ADR. This indicated that the sensitivity of breast cancer cells to ADR is associated with HIF1α and TFRC-mediated ferroptosis, and activating ferroptosis can significantly increase the sensitivity of breast cancer cells to ADR. However, given the ability of HIF1α to regulate a variety molecules involved in ferroptosis pathway, more evidence needs to be collected before the contribution of TFRC-mediated ferroptosis can be determined. The interactions between different target molecules should also be considered since HIF1α usually work through a complicated downstream network which includes more than a single target.

Our experimental results suggested that TFRC is regulated by the transcription factor HIF1α. To confirm this finding, we conducted dual-luciferase experiments and recorded a direct interaction between HIF1α and TFRC. HIF1α acts as a transcription factor for TFRC, initiating its transcription and influencing its expression. To further investigate the regulatory effect of HIF1α on TFRC expression and its impact on resistance mechanisms, we transduced the drug-resistant BT-549 cells with lentivirus to upregulate HIF1α. HIF1α upregulation was followed by a significant increase in TFRC, Fe^{2+}, and MDA levels in cells. Following combined treatment with ADR, cell viability decreased significantly, along with a significant decrease in IC50, as well as a substantial reduction in cell clonogenicity and invasion capability. To confirm that HIF1α-mediated upregulation of TFRC reverses ADR resistance by activating ferroptosis, we performed rescue experiments by co-treating with the ferroptosis inhibitor Fer-1. The results showed that Fer-1 rescued the cytotoxic effect of ADR on drug-resistant breast cancer cells after HIF1α was upregulated. The resistance of cells to ADR, IC50 values, cell proliferation, colony formation, and invasion capabilities were enhanced. These findings indicated that HIF1α acts as a positive upstream transcription factor of TFRC, upregulating TFRC expression, inducing Fe^{2+} overload, and activating ferroptosis in breast cancer-resistant cells. Thus, it significantly increases their sensitivity to ADR and reverses their resistance. It is worth noted that the regulatory mechanism of HIF1α on TFRC might not be that simple. Herein, we found that HIF1α acts as a transcription factor for TFRC, initiating its transcription and influencing its expression. However, it might not be the only way by which HIF1α regulates the expression of TFRC. A negative feedback loop can be formed between

PER1 and HIF1α to promote ferroptosis and inhibit tumor progression in oral squamous cell carcinoma, which also leads to alteration in TFRC expression.[36] In this study, PER1 was shown to exert a regulatory effect on the expression of TFRC, which is also regulated by a feedback mechanism that includes HIF1α. Therefore, it is reasonable to believe that the straight axis structure is only part of the regulatory machinery by which HIF1α regulates the expression of TFRC. It is reasonable to believe that a complicated network functions together to achieve this regulatory effect, which needs to be validated by more evidence.

To adapt to their environment, tumor cells develop complex metabolic mechanisms during malignant transformation, which increases tumor survival. The findings of our experiment showed that low expression of HIF1α in drug-resistant cells reflects this metabolic characteristic of tumors. HIF1α is upregulated in tumors under hypoxic conditions to alleviate hypoxia. However, our experimental results suggest that HIF1α in tumor cells exhibits different characteristics in chemotherapy resistance compared to the above. We speculated that this might be related to the unique environment and metabolic demands of drug-resistant cells. Unlike normal cells, tumor cells generate energy primarily through glycolysis even under aerobic conditions, a phenomenon known as the Warburg effect,[37] especially in highly malignant tumors, to meet the demands for rapid growth and proliferation under hypoxic conditions. The Warburg effect not only enhances the ability of tumor cells to survive under adverse conditions but also contributes to drug resistance. Enhancing glycolysis in tumor cells can increase the resistance of these cells to chemotherapeutic drugs.[38] We speculated that drug-resistant tumor cells, unlike general tumor cells, can survive in harsh environments because they have complex metabolic coordination mechanisms. Warburg effect occurs in ADR-resistant breast cancer cells; these cells do not rely on HIF1α to increase aerobic oxidation levels. In such cases, moderate downregulation of HIF1α ensures the low iron homeostasis needed by ADR-resistant cells. This avoids iron overload and, thus, mitigates the risk of ferroptosis triggered by the Fenton reaction induced by ADR, ensuring the survival of resistant cells. Therefore, upregulating HIF1α to induce the overexpression of TFRC and increase Fe^{2+} concentration, thereby activating ferroptosis, might be a novel and effective approach to reversing ADR resistance.

In conclusion, ferroptosis occurs in breast cancer and is related to drug resistance in breast cancer cells. Targeting HIF1α can regulate the transcription of TFRC, affect its expression, increase iron ion abundance, activate ferritin decarboxylase, and reverse cancer resistance to ADR. However, the mechanism of tumor drug resistance is complex, and our study provides preliminary information on the relationship between cancer ADR resistance and ferroptosis, as well as the regulatory mechanisms of HIF1α and TFRC, which highlights the correlation between hypoxia and ADR resistance in breast cancer and ferroptosis. The mechanism by which ferroptosis occurs is extremely complex, and the IREB2/TFRC/FTH1 iron ion metabolism pathway investigated in this study is only a part of a large process. Thus, further studies are needed to understand the mechanism underlying ferroptosis and its relationship with the Warburg effect. In addition, whether other key factors for ferroptosis are involved is not yet clear. More importantly, the hypoxic microenvironment of solid tumors is complicated. Using an in vitro cellular model might not fully represent real conditions. Therefore, in vivo models are needed to fully determine the role of HIF1α in ADR resistance in breast cancer and ferroptosis. On the other hand, it has been reported that the role of ferroptosis in ADR resistance might differ between ER+ and ER− breast cancer cells. Hence, different models need to be established to examine the underlying mechanisms and relevant regulatory factors involved.

AUTHOR CONTRIBUTIONS

Xiaojie Yu designed the study and performed editing and critical revision of this manuscript. Xiaojie Yu and Zhenlin Yang performed the experiments and analyzed the data. Qingqun Guo and Xiaohong Wang collected the samples. Yong Han, Hao Zhangjie, and Xiaohong Wang classified the samples. All authors read and approved the final manuscript.

ACKNOWLEDGMENTS

We thank Feifei Wen for professional pathological assistance, including diagnosis and immunohistochemical analysis.

FUNDING INFORMATION

This work was supported by National Natural Science Foundation of China (No. 81902702), Natural Science Foundation of Shandong Province (No. ZR2023MH115 and ZR2017LH072), and National Key Research and Development Project (No. 2018YFC0114705).

DISCLOSURES

The authors declare that they have no known competing financial interests or personal relationships that could have appeared to influence the work reported in this paper. I would like to declare on behalf of my coauthors that this work was original research that has not been published previously, and not under consideration for publication elsewhere in whole or in part.

DATA AVAILABILITY STATEMENT

The data sets presented in this study can be found in online repositories. The names of the repository/repositories and accession number(s) can be found in the article. And all the data are real and available.

ETHICS APPROVAL AND CONSENT TO PARTICIPATE

The studies involving human participants were reviewed and approved by Medical Research Ethics Committee of Binzhou Medical University Hospital (Approval No. LW-178). The patients/participants provided their written informed consent to participate in this study.

ORCID

Xiaojie Yu https://orcid.org/0009-0000-4420-0555
Qingqun Guo https://orcid.org/0009-0008-9926-8846
Haojie Zhang https://orcid.org/0009-0000-1100-8663
Xiaohong Wang https://orcid.org/0000-0002-4558-7349
Yong Han https://orcid.org/0000-0002-2550-3072
Zhenlin Yang https://orcid.org/0000-0002-5409-9697

REFERENCES

1. Chen NN, Ma XD, Miao Z, et al. Doxorubicin resistance in breast cancer is mediated via the activation of FABP5/PPARgamma and CaMKII signaling pathway. *Front Pharmacol*. 2023;14:1150861. doi:10.3389/fphar.2023.1150861
2. Zhao L, Zhou X, Xie F, et al. Ferroptosis in cancer and cancer immunotherapy. *Cancer Commun*. 2022;42(2):88-116. doi:10.1002/cac2.12250
3. Chen X, Li J, Kang R, Klionsky DJ, Tang D. Ferroptosis: machinery and regulation. *Autophagy*. 2021;17(9):2054-2081. doi:10.1080/15548627.2020.1810918
4. Gao M, Monian P, Quadri N, Ramasamy R, Jiang X. Glutaminolysis and transferrin regulate ferroptosis. *Mol Cell*. 2015;59(2):298-308. doi:10.1016/j.molcel.2015.06.011
5. Wang X, Cheng K, Zhang G, et al. Enrichment of CD44 in exosomes from breast cancer cells treated with doxorubicin promotes chemoresistance. *Front Oncol*. 2020;10:960. doi:10.3389/fonc.2020.00960
6. Wang Y, Liu Y, Liu J, Kang R, Tang D. NEDD4L-mediated LTF protein degradation limits ferroptosis. *Biochem Biophys Res Commun*. 2020;531(4):581-587. doi:10.1016/j.bbrc.2020.07.032
7. Wang X, Wang Y, Huang D, et al. Astragaloside IV regulates the ferroptosis signaling pathway via the Nrf2/SLC7A11/GPX4 axis to inhibit PM2.5-mediated lung injury in mice. *Int Immunopharmacol*. 2022;112:109186. doi:10.1016/j.intimp.2022.109186
8. Xiong Q, Li X, Li W, et al. WDR45 mutation impairs the autophagic degradation of transferrin receptor and promotes ferroptosis. *Front Mol Biosci*. 2021;8:645831. doi:10.3389/fmolb.2021.645831
9. Kuang F, Liu J, Tang D, Kang R. Oxidative damage and antioxidant defense in ferroptosis. *Front Cell Dev Biol*. 2020;8:586578. doi:10.3389/fcell.2020.586578
10. Pinnix ZK, Miller LD, Wang W, et al. Ferroportin and iron regulation in breast cancer progression and prognosis. *Sci Transl Med*. 2010;2(43):43ra56. doi:10.1126/scitranslmed.3001127
11. Wang W, Deng Z, Hatcher H, et al. IRP2 regulates breast tumor growth. *Cancer Res*. 2014;74(2):497-507. doi:10.1158/0008-5472.CAN-13-1224
12. Yu X, Cheng L, Liu S, et al. Correlation between ferroptosis and adriamycin resistance in breast cancer regulated by transferrin receptor and its molecular mechanism. *FASEB J*. 2024;38(5):e23550. doi:10.1096/fj.202302597R
13. Henning Y, Blind US, Larafa S, Matschke J, Fandrey J. Hypoxia aggravates ferroptosis in RPE cells by promoting the Fenton reaction. *Cell Death Dis*. 2022;13(7):662. doi:10.1038/s41419-022-05121-z
14. Zhang J, Yang J, Zuo T, et al. Heparanase-driven sequential released nanoparticles for ferroptosis and tumor microenvironment modulations synergism in breast cancer therapy. *Biomaterials*. 2021;266:120429. doi:10.1016/j.biomaterials.2020.120429
15. Zeng L, Ding S, Cao Y, et al. A MOF-based potent ferroptosis inducer for enhanced radiotherapy of triple negative breast cancer. *ACS Nano*. 2023;17(14):13195-13210. doi:10.1021/acsnano.3c00048
16. Stockwell BR, Friedmann AJ, Bayir H, et al. Ferroptosis: a regulated cell death nexus linking metabolism, redox biology, and disease. *Cell*. 2017;171(2):273-285. doi:10.1016/j.cell.2017.09.021
17. Dixon SJ, Lemberg KM, Lamprecht MR, et al. Ferroptosis: an iron-dependent form of nonapoptotic cell death. *Cell*. 2012;149(5):1060-1072. doi:10.1016/j.cell.2012.03.042
18. Hentze MW, Muckenthaler MU, Andrews NC. Balancing acts: molecular control of mammalian iron metabolism. *Cell*. 2004;117(3):285-297. doi:10.1016/s0092-8674(04)00343-5
19. Zhou H, Chen J, Fan M, et al. KLF14 regulates the growth of hepatocellular carcinoma cells via its modulation of iron homeostasis through the repression of iron-responsive element-binding protein 2. *J Exp Clin Cancer res*. 2023;42(1):5. doi:10.1186/s13046-022-02562-4
20. Xia H, Wu Y, Zhao J, et al. N6-Methyladenosine-modified circSAV1 triggers ferroptosis in COPD through recruiting YTHDF1 to facilitate the translation of IREB2. *Cell Death Differ*. 2023;30(5):1293-1304. doi:10.1038/s41418-023-01138-9
21. Lu Y, Yang Q, Su Y, et al. MYCN mediates TFRC-dependent ferroptosis and reveals vulnerabilities in neuroblastoma. *Cell Death Dis*. 2021;12(6):511. doi:10.1038/s41419-021-03790-w
22. Wang X, Wu R, Zhai P, et al. Hypoxia promotes EV secretion by impairing lysosomal homeostasis in HNSCC through negative regulation of ATP6V1A by HIF-1alpha. *J Extracell Vesicles*. 2023;12(2):e12310. doi:10.1002/jev2.12310
23. Schito L, Semenza GL. Hypoxia-inducible factors: master regulators of cancer progression. *Trends Cancer*. 2016;2(12):758-770. doi:10.1016/j.trecan.2016.10.016
24. Song S, Zhang G, Chen X, et al. HIF-1alpha increases the osteogenic capacity of ADSCs by coupling angiogenesis and osteogenesis via the HIF-1alpha/VEGF/AKT/mTOR signaling pathway. *J Nanobiotechnology*. 2023;21(1):257. doi:10.1186/s12951-023-02020-z
25. Zhang Z, Qiu L, Lin C, et al. Copper-dependent and -independent hypoxia-inducible factor-1 regulation of gene expression. *Metallomics*. 2014;6(10):1889-1893. doi:10.1039/c4mt00052h

26. Wang Q, Zhou M, Zhang H, Hou Z, Liu D. Hypoxia treatment of adipose mesenchymal stem cells promotes the growth of dermal papilla cells via HIF-1alpha and ERK1/2 signaling pathways. *Int J Mol Sci*. 2023;24(13):11198. doi:10.3390/ijms241311198
27. Zhao Y, Xing C, Deng Y, Ye C, Peng H. HIF-1alpha signaling: essential roles in tumorigenesis and implications in targeted therapies. *Genes dis*. 2024;11(1):234-251. doi:10.1016/j.gendis.2023.02.039
28. Wicks EE, Semenza GL. Hypoxia-inducible factors: cancer progression and clinical translation. *J Clin Invest*. 2022;132(11):e159839. doi:10.1172/JCI159839
29. Zou Y, Palte MJ, Deik AA, et al. A GPX4-dependent cancer cell state underlies the clear-cell morphology and confers sensitivity to ferroptosis. *Nat Commun*. 2019;10(1):1617. doi:10.1038/s41467-019-09277-9
30. Sun S, Guo C, Gao T, et al. Hypoxia enhances glioma resistance to sulfasalazine-induced ferroptosis by upregulating SLC7A11 via PI3K/AKT/HIF-1alpha Axis. *Oxidative Med Cell Longev*. 2022;2022:7862430. doi:10.1155/2022/7862430
31. Zhu Y, Yang L, Yu Y, et al. Hydroxysafflor yellow a induced ferroptosis of osteosarcoma cancer cells by HIF-1alpha/HK2 and SLC7A11 pathway. *Oncol Res*. 2024;32(5):899-910. doi:10.32604/or.2023.042604
32. Yang Z, Su W, Wei X, et al. HIF-1alpha drives resistance to ferroptosis in solid tumors by promoting lactate production and activating SLC1A1. *Cell Rep*. 2023;42(8):112945. doi:10.1016/j.celrep.2023.112945
33. Chen C, Hao X, Geng Z, Wang Z. ITRAQ-based quantitative proteomic analysis of MG63 in response to HIF-1alpha inducers. *J Proteome*. 2020;211:103558. doi:10.1016/j.jprot.2019.103558
34. Ozgur B, Helms H, Tornabene E, Brodin B. Hypoxia increases expression of selected blood-brain barrier transporters GLUT-1, P-gp, SLC7A5 and TFRC, while maintaining barrier integrity, in brain capillary endothelial monolayers. *Fluids Barriers CNS*. 2022;19(1):1. doi:10.1186/s12987-021-00297-6
35. Pan Y, Yang J, Dai J, Xu X, Zhou X, Mao W. TFRC in cardiomyocytes promotes macrophage infiltration and activation during the process of heart failure through regulating Ccl2 expression mediated by hypoxia inducible factor-1alpha. *Immun Inflamm Dis*. 2023;11(8):e835. doi:10.1002/iid3.835
36. Yang Y, Tang H, Zheng J, Yang K. The PER1/HIF-1alpha negative feedback loop promotes ferroptosis and inhibits tumor progression in oral squamous cell carcinoma. *Transl Oncol*. 2022;18:101360. doi:10.1016/j.tranon.2022.101360
37. Barba I, Carrillo-Bosch L, Seoane J. Targeting the Warburg effect in cancer: where do we stand? *Int J Mol Sci*. 2024;25(6):3142. doi:10.3390/ijms25063142
38. Fan K, Fan Z, Cheng H, et al. Hexokinase 2 dimerization and interaction with voltage-dependent anion channel promoted resistance to cell apoptosis induced by gemcitabine in pancreatic cancer. *Cancer Med*. 2019;8(13):5903-5915. doi:10.1002/cam4.2463

SUPPORTING INFORMATION

Additional supporting information can be found online in the Supporting Information section at the end of this article.

How to cite this article: Yu X, Guo Q, Zhang H, Wang X, Han Y, Yang Z. Hypoxia-inducible factor-1α can reverse the Adriamycin resistance of breast cancer adjuvant chemotherapy by upregulating transferrin receptor and activating ferroptosis. *The FASEB Journal*. 2024;38:e23876. doi:10.1096/fj.202401119R